Molecular Therapy
Nucleic Acids
Original Article

Targeting TLR9 agonists to secondary lymphoid organs induces potent immune responses against HBV infection

Irina Ushach,[1] Ren Zhu,[1,2] Elen Rosler,[1] Rajendra K. Pandey,[1] N. Tilani S. De Costa,[1] Soheil Pourshahian,[1] Qinglin Han,[1,2] Chris Li,[1,2] Leonid Beigelman,[1] Sergei M. Gryaznov,[1] and Theodore Yun[1]

[1]Janssen Pharmaceutical Companies of Johnson & Johnson, 260 E. Grand Avenue, 169 Harbor Boulevard, South San Francisco, CA 94080, USA; [2]China R&D, Janssen Pharmaceuticals, 4560 Jinke Road, Pudong, Shanghai 200010, China

Despite the existence of a prophylactic vaccine against hepatitis B virus (HBV), chronic hepatitis B virus (CHB) infection remains the leading cause of cirrhosis and liver cancer in developing countries. Because HBV persistence is associated with insufficient host immune responses to the infection, development of an immunomodulator as a component of therapeutic vaccination may become an important strategy for treatment CHB. In the present study, we aimed to design a novel immunomodulator with the capacity to subvert immune tolerance to HBV. We developed a lymphoid organ-targeting immunomodulator by conjugating a naturally occurring, lipophilic molecule, α-tocopherol, to a potent CpG oligonucleotide adjuvant pharmacophore. This approach resulted in preferential trafficking of the α-tocopherol-conjugated oligonucleotide to lymphoid organs where it was internalized by antigen-presenting cells (APCs). Moreover, we show that conjugation of the oligonucleotides to α-tocopherol results in micelle-like structure formation, which improved cellular internalization and enhanced immunomodulatory properties of the conjugates. In a mouse model of chronic HBV infection, targeting CpG oligonucleotide to lymphoid organs induced strong cellular and humoral immune responses that resulted in sustained control of the virus. Given the potency and tolerability of an α-tocopherol-conjugated CpG oligonucleotide, this modality could potentially be broadly applied for therapeutic vaccine development.

INTRODUCTION

More than 350 million people worldwide are affected by chronic hepatitis B virus (CHB) infection which is associated with complications due to development of cirrhosis or hepatocellular carcinoma.[1] Current treatment options for CHB infection include type I interferon (IFN) (e.g., Pegasys) and antiviral nucleosides, which suppress viral replication. In general, these therapies are unable to provide lasting antiviral immunity or viral clearance. Furthermore, such therapies require life-long administration and are often hampered by tolerability concerns, virus drug resistance, and escape mutant virus.[2,3] Therefore, development of novel therapies that would allow control and clearance of CHB infection is urgently needed. CHB infection is characterized by unresponsive immune responses to the infection. In a self-limiting infection, hepatitis B virus (HBV)-specific T cells exhibit strong T-helper 1 (Th1)-associated immune responses that result in efficient control of infection and successful maturation of T cell memory.[4,5] In patients with CHB infection, however, the HBV-specific T cell response is very weak, and prolonged expression of HBV antigens often results in functional inactivation and deletion of HBV-specific T cells.[6,7]

Toll-like receptors (TLRs) play a critical role in pathogen recognition and serve as an important link between innate and adaptive immune systems. In animal models, reactivation of immune system through pharmacological stimulation of endosomal TLRs such as TLR3, TLR7/8, or TLR9 have been shown to be protective against HBV infection.[8] Oligonucleotides containing unmethylated cytosine-guanine (CpG) motifs are recognized by TLR9 receptors in endosomes of immune cells such as plasmacytoid dendritic cells (pDCs) and B cells in human, and pDCs, dendritic cells (DCs), monocytes, and B cells in mouse.[9] Activation of TLR9 receptors biases the immune response toward type 1 with the production of a Th1-like pattern of cytokines, such as IFNs, tumor necrosis factor alpha (TNFα) and interleukin (IL)-12, B cell proliferation, and immunoglobulin (Ig) G class switching.[10] Several variations of therapeutic and prophylactic vaccines containing TLR9 agonists are currently in clinical trials where these immunomodulatory approaches show promising results against numerous cancer and infectious indications.[11]

In this report, we describe a novel and effective TLR9 immunomodulatory agonist that stimulates human and mouse TLR9 (mTLR9)-expressing cells *in vitro* and *in vivo*. Because immune responses to a pathogen are initiated and orchestrated in secondary lymphoid organs, we hypothesized that targeting TLR9 agonists to these organs

Received 23 August 2021; accepted 28 January 2022;
https://doi.org/10.1016/j.omtn.2022.01.020.

Correspondence: Irina Ushach, 260 E. Grand Avenue, 169 Harbor Boulevard, South San Francisco, CA 94080, USA
E-mail: iushach@its.jnj.com

would result in enhanced efficacy of the immune response against HBV infection. Several strategies for efficient delivery of compounds to lymphoid tissues have been described, such as using nanoparticles, drug-loaded liposomes, and compounds conjugated to lipids.[12,13] In the current report, we describe a novel strategy to conjugate CpG oligonucleotides to α-tocopherol (Toco; vitamin E) using a cleavable linker. We found that α-tocopherol imparted highly desirable biophysical properties to the oligonucleotides, such as assembling into micellular-like structures and binding to albumin. α-Tocopherol-conjugated CpG oligonucleotides had improved cellular internalization kinetics and enhanced immunostimulatory properties. Furthermore, when administered *in vivo*, α-tocopherol-conjugated CpG oligonucleotides were transported more efficiently to secondary lymphoid tissues (i.e., spleen and lymph nodes), where they were internalized by APCs. By targeting of CpG oligonucleotides to immune organs, we observed enhanced immune responses in an adjuvant model and improved efficacy in the adeno-associated virus (AAV)/HBV model of CHB infection that led to a sustained control of viral load, even after discontinuation of treatment.

RESULTS

Designing a novel and more potent TLR9 agonists

The ability of oligonucleotides to bind and activate TLR9 depends on its sequence and sugar-phosphate backbone chemistry.[14] To date, immunomodulatory CpG oligonucleotides have been broadly categorized into four classes based on similarities between biological and structural properties.[10] Among them, K-type oligonucleotides (also referred to as class B oligonucleotides) contain a full phosphorothioate (PS) backbone and one or more CpG dinucleotides. They trigger signaling in APCs that leads to potent type 1 innate and adaptive immune responses. As powerful immunomodulators, CpG oligonucleotides have been developed as vaccine adjuvants or immunotherapeutics for infectious diseases or cancer indications.

In clinical trials, the class B oligonucleotide ODN2006 (also known as ODN7909), which activates human TLR9, has been shown to be protective against a variety of viral infections, and another class B oligonucleotide is now approved as part of a vaccine for HBV prevention.[15] In this present study, our goal was to develop a novel, potent TLR9 agonist that could be targeted to secondary lymphoid organs whereby the TLR9 agonist would further enhance its effect on modulating the immune response. The three-dimensional structure of TLR9 complexed to an agonist oligonucleotide revealed that the residues of the receptor interacted with the phosphate of the backbone between cytosine and guanosine of the CpG motif.[16] We explored modifications in the oligonucleotide backbone structure by reverting the PS molecule at each CpG motif back to the native phosphodiester (PO) and investigating whether these reversions could affect the stimulatory properties of the oligonucleotide.

We synthesized a series of compounds based on the prototypic class B molecule ODN7909 and found that placement of PO in at least two out its four CpG motifs substantially increased nuclear factor κB (NF-κB) activation in the HEK-Blue hTLR9 reporter cell line (Figure 1). When all four CpG motifs are linked with a PO backbone (PO-CpG oligonucleotide), there is a 2-fold enhancement in maximum activity, and a 3-fold decrease in half maximal effective concentration (EC50) value (Figure 1A). By sequentially modifying the backbone PO at each, or in a combination of two or more CpG motifs, we determined that positioning PO linkages in the second and third CpG motifs potentiates oligonucleotide activity (Figure 1B). Although the optimal nucleotide sequence for activating TLR9 varies among species, some CpG agonists can cross-react between TLR9 receptors from different species. ODN7909 (PS-CpG), for example, can weakly stimulate mTLR9. We tested the activity of PO-CpG on mTLR9 using the related reporter cell line, HEK-Blue mTLR9. Interestingly, while ODN7909 weakly activates mTLR9, PO-CpG activates mTLR9 with a similar potency to the mouse specific TLR9 agonist, ODN1826 (Figure 1C).

Conjugation of CpG oligonucleotides to a lipophilic moiety enhances their immunomodulatory activity

Trafficking of immune cells and transport of antigens throughout the circulatory system is essential for pathogen recognition and initiation of an immune response to an infection. We hypothesized that targeting CpG oligonucleotides to secondary lymphoid tissues would efficiently activate APCs and stimulate increased protection against HBV. Multiple strategies for delivering drugs to lymphoid organs have been described, including drug-loaded liposomes, nanoparticles, micelles, and drug conjugated to a lipophilic tail.[12,13,17] Ideally, a lymphatic targeted drug delivery system should meet the following criteria: lead to a high uptake and accumulation of a drug in lymphoid organs, exhibit drug release from the delivery system properties, and show a low toxicity profile. The lipophilic α-tocopherol molecule is well tolerated and is neither mutagenic nor carcinogenic even at high doses.[18] Moreover, Radovic-Moreno et al. demonstrated that α-tocopherol conjugation to the mTLR9-specific agonist ODN1826 enhances its *in vitro* and *in vivo* properties.[12] Similarly, Liu et al. demonstrated that, by conjugating a CpG oligonucleotide to a synthetic lipid, the biodistribution properties were altered and the oligonucleotide was preferentially delivered to the lymph nodes (LNs) after subcutaneous (SC) injection.[13]

To address these criteria, we conjugated a cleavable (under endosomal localization conditions) linker, which connects the lipid targeting moiety to the CpG oligonucleotide pharmacophores. Two hydrophilic hexaethylene glycol groups were connected to each other and to the oligonucleotide pharmacophore via natural PO groups. As immune organ-targeting moieties, we initially selected two naturally occurring lipophilic molecules, cholesterol (Chol) and α-tocopherol. We rationalized that the presence of relatively unstable phosphodiester groups in the linker should allow oligonucleotide pharmacophore release in endosomal compartments. The lipids were attached to the 5′-terminus of the oligonucleotide (Figure 2A). This strategy preserved agonist activity against both human TLR9 and mTLR9 in HEK cell reporter assay (Figures 2B and 2C). Moreover, PO-CpGs conjugated to the lipophilic moiety were more potent at inducing proinflammatory cytokine production, including IFNα, TNFα, and IL-6, by

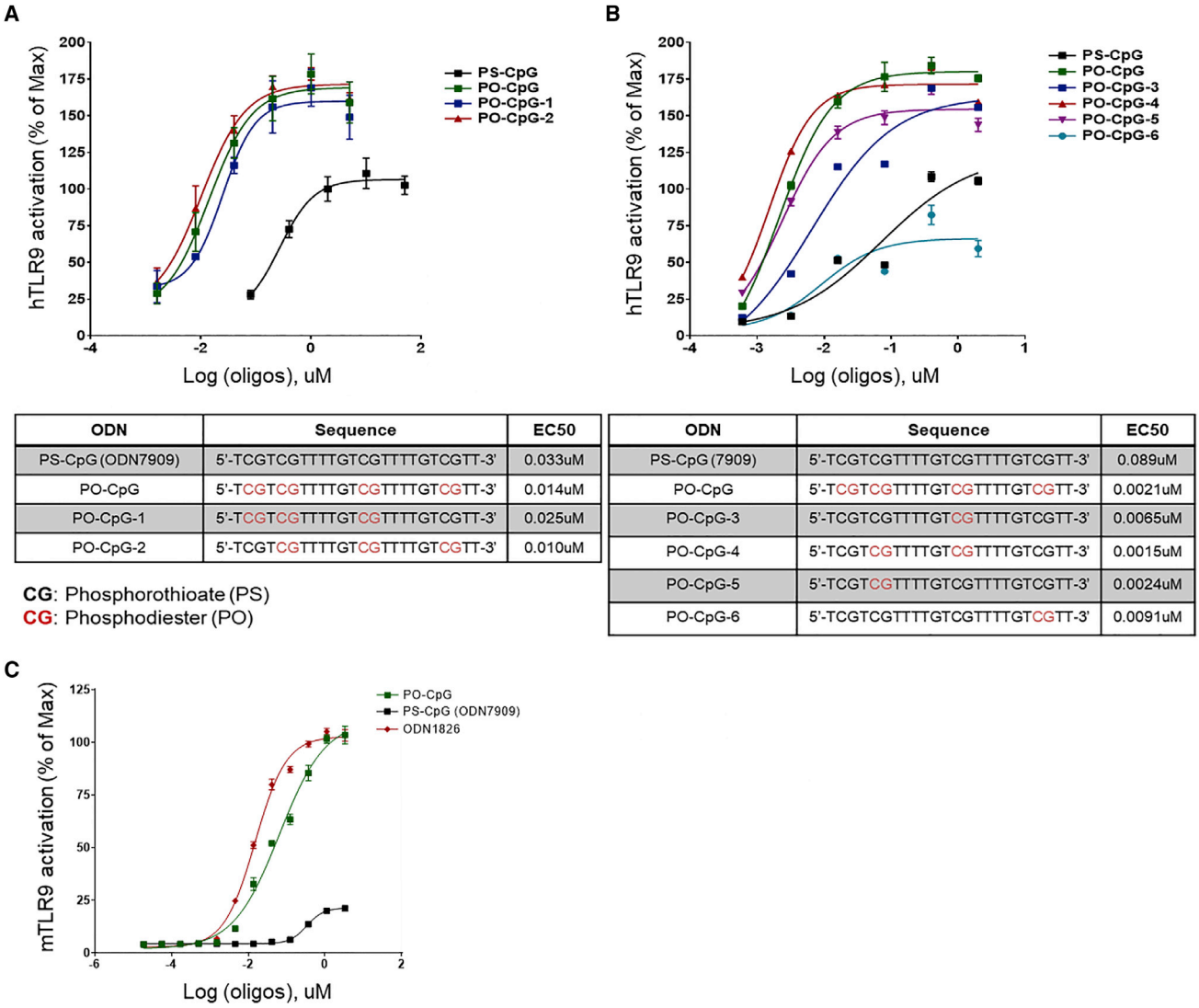

ODN	Sequence	EC50
PS-CpG (ODN7909)	5'-TCGTCGTTTTGTCGTTTTGTCGTT-3'	0.033uM
PO-CpG	5'-TCGTCGTTTTGTCGTTTTGTCGTT-3'	0.014uM
PO-CpG-1	5'-TCGTCGTTTTGTCGTTTTGTCGTT-3'	0.025uM
PO-CpG-2	5'-TCGTCGTTTTGTCGTTTTGTCGTT-3'	0.010uM

CG: Phosphorothioate (PS)
CG: Phosphodiester (PO)

ODN	Sequence	EC50
PS-CpG (7909)	5'-TCGTCGTTTTGTCGTTTTGTCGTT-3'	0.089uM
PO-CpG	5'-TCGTCGTTTTGTCGTTTTGTCGTT-3'	0.0021uM
PO-CpG-3	5'-TCGTCGTTTTGTCGTTTTGTCGTT-3'	0.0065uM
PO-CpG-4	5'-TCGTCGTTTTGTCGTTTTGTCGTT-3'	0.0015uM
PO-CpG-5	5'-TCGTCGTTTTGTCGTTTTGTCGTT-3'	0.0024uM
PO-CpG-6	5'-TCGTCGTTTTGTCGTTTTGTCGTT-3'	0.0091uM

Figure 1. Designing structurally optimized CpG oligonucleotide

(A and B) Screen of a series of compounds with PO-CpG pharmacophore placed in various CpG motifs in human HEK 293 reporter cell line. (C) Culturing HEK cells with PO-CpG oligonucleotide results in NF-κB activation in both human (A and B) and mouse (C) reporter cell lines.

primary human peripheral blood mononuclear cells (PBMCs) (Figures 2D–2G). Screening of cholesterol and α-tocopherol-conjugated oligonucleotides in control TLR2, 3, 4, 5, 7, and 8 HEK cell reporter cell lines indicated that the increase in activity was not due to activation of other TLRs, ruling out a direct adjuvant effect of the lipid moieties (Figure S1). It is important to note that 5′ conjugation of lipid groups to the CpG oligonucleotide pharmacophores via non-cleavable linker essentially abrogates the compounds' activity (Figure S2).

Because the cholesterol- or α-tocopherol-conjugated CpG oligonucleotides were equally effective at stimulating human TLR9 and mTLR9, and because it has been previously demonstrated that α-tocopherol-conjugated, mTLR9-specific CpG oligonucleotide had enhanced efficacy *in vitro*,[12] we wanted to determine how these conjugated CpG oligonucleotides affected immune cell activation *in vivo* in mice. We administered PO-CpG, cholesterol-conjugated PO-CpG (Chol-PO-CpG) or α-tocopherol-conjugated PO-CpG (Toco-PO-CpG) in mice either intravenously (IV) or SC and then monitored the kinetics of serum cytokine induction over 48 h post dose. We found that all oligonucleotides resulted in similar kinetics of cytokine production regardless of administration route: rapid increase 30 min post delivery with most cytokine levels peaking around 1–4 h and subsiding back to a basal level by 12 h (Figures 2H–2M). The effect of conjugation of oligonucleotides to lipophilic moieties varied from cytokine to cytokine, although we found that IV administration of Toco-PO-CpG and Chol-PO-CpG resulted in enhanced production of several

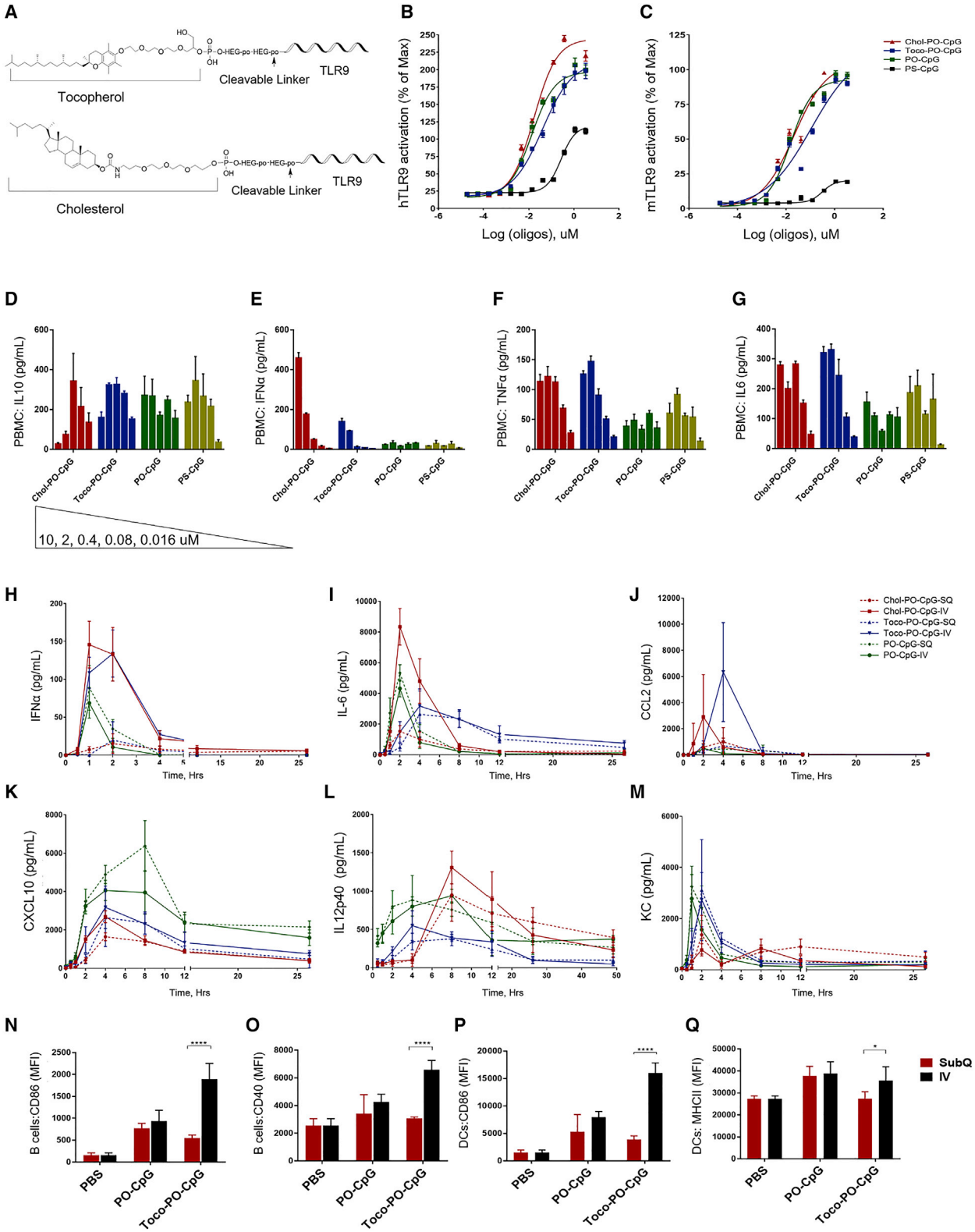

(legend on next page)

proinflammatory cytokines and chemokines, including IFNα and CCL2 (Figures 2H–2M). Moreover, analysis of several activation markers, including cluster of differentiation (CD) 86, CD40, and major histocompatibility complex (MHC) II, expressed on B cells and DCs 24 h post treatment revealed significantly stronger activation of APCs in Toco-PO-CpG-treated mice when compared with PO-CpG-treated animals (Fig.2N-Q). All *in vivo* experiments were performed at least twice and showed comparable results. Although all conjugated compounds we tested were generally well tolerated, we decided to focus on α-tocopherol-conjugated oligonucleotides for further *in vivo* testing.

Tocopherol-conjugated CpG oligonucleotides form micellar-like structures that improve their cell internalization kinetics

Previously, it has been shown that conjugation of oligonucleotides to a fatty acid results in the formation of micellar structures, which improved their cellular internalization properties.[12,19] We, therefore, investigated whether conjugation of α-tocopherol to the oligonucleotide increased cellular internalization through micelle formation and, therefore, could account for enhanced biological activity. To determine whether 5′-α-tocopherol-conjugated CpG oligonucleotides form micelle-like structures, we performed size-exclusion chromatography (SEC) studies, where molecular aggregation status (i.e., presence of monomeric or multimeric forms) of the oligonucleotides were assessed. Conjugated and unconjugated oligonucleotides have a similar size and, therefore, monomeric forms are expected to have similar retention times in SEC. We found that the conjugated oligonucleotide had a shorter retention time and eluted faster from the column than its unconjugated form (Figure 3A). It was hypothesized that the shorter retention time of the conjugated CpG is due to the formation of micellar-like structures with higher molecular weights corresponding to the oligonucleotide in its multimeric form. To confirm the presence of micellar-like structures, samples were prepared in the presence or absence of urea in phosphate-buffered saline (PBS) solutions and analyzed by SEC. It has been reported that urea efficiently disrupts macromolecular micellular structures.[20] Figure 3A shows that the SEC retention time of unconjugated PO-CpG oligonucleotide was not affected by urea, indicating a lack of micelle formation. In contrast, the retention time for carboxyfluorescein (FAM)-labeled Toco-PO-CpG conjugate shifted to a higher value in the presence of urea, consistent with the disruption of micellar-like structures by urea.

Liu et al. demonstrated that conjugation of a synthetic lipid to an oligonucleotide resulted in enhanced biodistribution to secondary LNs due to its ability to bind to albumin.[13] Because α-tocopherol is a lipophilic molecule, we wanted to determine whether conjugation of oligonucleotides to α-tocopherol could also affect its albumin binding ability. We tested the interaction of BSA with FAM-labeled CpG oligonucleotides by SEC. BSA exhibited a major chromatographic peak eluting at 13.2 min (Figure 3B). FAM-labeled PO-CpG oligonucleotide eluted as a monomer at 17 min either in the presence or absence of BSA, indicating lack of binding to albumin. FAM-labeled Toco-PO-CpG eluted faster than PO-CpG at 11.8 min, demonstrating that it forms higher-molecular-weight structures, consistent with the previous observations (Figure 3A). After incubation with albumin, FAM-labeled Toco-PO-CpG co-migrated with BSA, indicating that it is bound to this molecule (Figure 3B). Together, these results demonstrate α-tocopherol conjugation leads to the formation of micellar-type structures and enhancement of oligonucleotide albumin binding properties.

To confirm that the biophysical changes of α-tocopherol conjugation improved cellular internalization properties of oligonucleotides, we conjugated control PO-CpG or Toco-PO-CpG oligonucleotides to a fluorescent dye Alexa Fluor 647 (AF647) and measured their internalization efficiency in HEK-Blue hTLR9 cells using flow cytometry. Cells were incubated with oligonucleotides and then harvested at various time points up to 24 h. The cellular kinetics of oligonucleotide uptake were measured by the increase in mean fluorescent intensity (MFI) over time. The differences between the Toco-PO-CpG and PO-CpG uptake were observed as early as 15 min and, after 24 h, HEK-Blue hTLR9 cells had taken up approximately double the amount of Toco-PO-CpG oligonucleotide relative to the control (Figures 3C and 3D). We also assessed an uptake of fluorescently labeled CpG ODNs in mouse splenic B cells and DCs and, consistent with what we observed in the HEK-Blue cell line, tocopherol-conjugated CpG oligonucleotide was internalized more efficiently by these cells (Figure S3). Thus, conjugation of CpG oligonucleotides to α-tocopherol substantially enhanced their cellular uptake.

Tocopherol conjugation targets oligonucleotides to the secondary lymphoid tissues

Because lipid-conjugated oligonucleotides bound to albumin and Liu et al. demonstrated that this alteration enhanced its biodistribution to lymphoid tissues,[13] we asked whether α-tocopherol conjugation could also affect *in vivo* trafficking of CpG oligonucleotides. In order to visualize differences in biodistribution, we labeled Toco-PO-CpG and control PO-CpG oligonucleotides to AF647, which permitted real-time imaging of the oligonucleotide biodistribution using the *in vivo*

Figure 2. Lipid-conjugated CpG oligonucleotides demonstrate increased *in vitro* and *in vivo* potency

(A) Design of TLR9 agonist conjugated to a lipid moiety (tocopherol or cholesterol) via cleavable linker. (B and C) The activity of lipid-conjugated PO-CpG oligonucleotides and unmodified PO-CpG and PS-CpG oligonucleotides has been tested using human HEK-Blue TLR9 cells and (C) mouse HEK-Blue TLR9 reporter cell line. (D–G) Tocopherol- and cholesterol-conjugated PO-CpG oligonucleotides were more potent at inducing proinflammatory cytokines including IFNα, TNFα, and IL-6. (H–M) Lipid-conjugated or unmodified CpG oligonucleotides were administered in mice (n = 5 mice per group) through either IV or SC routes at the dose of 30 nmol/mouse. At various time points, serum samples were collected and tested for cytokines using multiplex panels. (N–Q) Toco-PO-CpG or PO-CpG oligonucleotides were administered in mice (n = 5) through either IV or SC routes (30nmol/mouse) and, 24 h post injections, spleens were collected for measurement of activation markers expressed on B cells (N and O) and DCs (P and Q). ****$p < 0.0001$, ***$p < 0.001$, **$p < 0.01$, *$p < 0.05$.

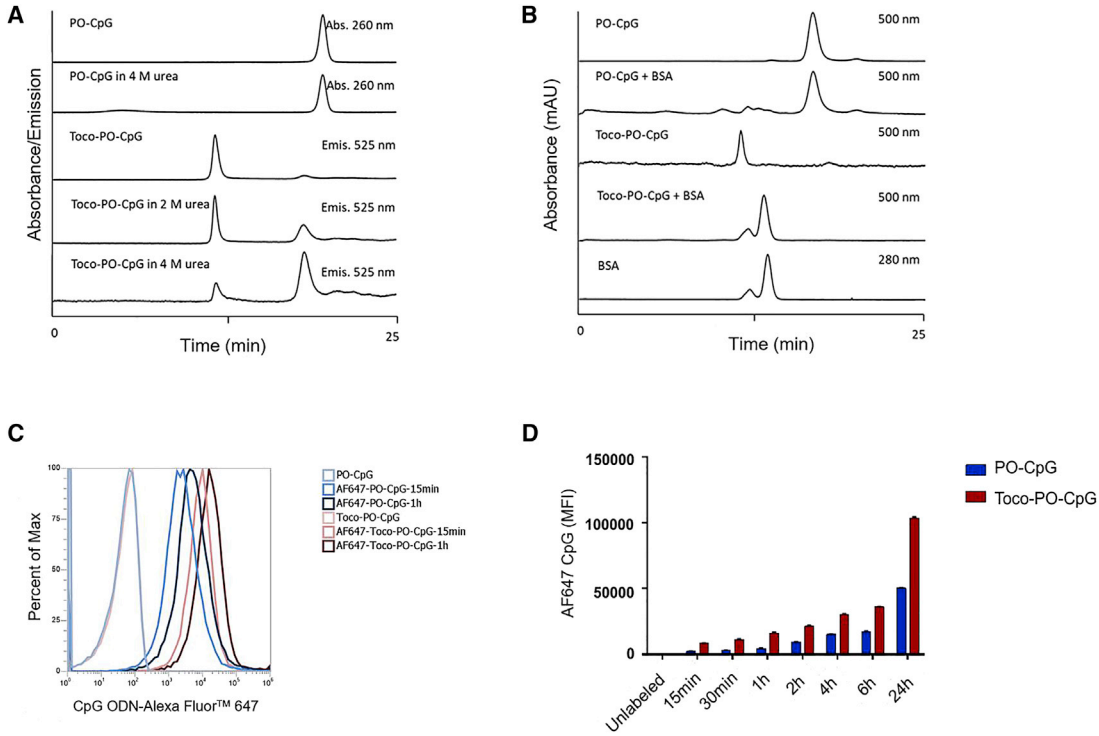

Figure 3. α-Tocopherol-conjugated CpG oligonucleotides form micelle structures

(A) SEC of FAM-labeled PO-CpG and Toco-PO-CpG oligonucleotides in the presence or absence of urea. The UV absorption chromatograms were recorded at 260 nm, while emission was recorded at 500 nm (excitation wavelength was 525 nm). In the absence of urea, Toco-PO-CpG elutes from the column faster that PO-CpG, which means it forms higher-molecular-weight species or micelles. In the presence of 2 M urea, some of these micelles are disrupted and a second peak with a similar retention time to the PO-CpG appears. Intensity of the second peak increases as concentration of urea is increased to 4 M, due to further disruption of micelles. (B) SEC of PO-CpG and Toco-PO-CpG in the presence or absence of BSA. The absorption chromatograms were recorded at 280 or 500 nm. The Toco-PO-CpG oligonucleotide binds to BSA, but PO-CpG does not. Toco-PO-CpG oligonucleotide elutes faster than PO-CpG, indicating that it forms higher-molecular-weight structures. (C) Histogram showing fluorescent intensity of cells incubated with AF647-labeled PO-CpG and Toco-PO-CpG oligonucleotides (1 μM) for 15 min and 1 h. (D) HEK 293 cells are cultured with AF647-labeled PO-CpG or Toco-PO-CpG at 1 μM concentration. At different time points, the cellular uptake of oligonucleotides was measured by flow cytometry.

imaging system (IVIS) and immunofluorescence (IF) microscopy. To determine whether AF647-modified oligonucleotides retain TLR9 stimulatory activity, we compared the activity of PO-CpG, Toco-PO-CpG, AF647-PO-CpG, and AF647-Toco-PO-CpG in HEK TLR9 reporter cell line and found that conjugation of oligonucleotides to AF647 fluorophore did not affect their activity (Figure S4). AF647-labeled Toco-PO-CpG and control PO-CpG oligonucleotides were injected either SC or IV in C57BL/6 mice and, 24 h post injections, draining LNs and spleens were excised for imaging. Following SC injections, unconjugated PO-CpG oligonucleotides showed slight uptake in draining LNs and spleens (Figures 4A and 4B). By contrast, accumulation of Toco-PO-CpG oligonucleotides was 2-fold higher in draining LNs than that of unconjugated PO-CpG oligonucleotides (Figure 4A and Figure S5). Following IV injections, both PO-CpG and Toco-PO-CpG oligonucleotides showed only marginal uptake in LNs (Figure 4A). In spleens, however, the accumulation of Toco-PO-CpG was 6-fold higher than that of its unconjugated counterpart (Figure 4B). Consistent with IVIS data, immunofluorescent staining revealed accumulation of Toco-PO-CpG oligonucleotide in draining LNs following SC injection (Figure 4C) and in spleens following IV injections (Figure 4D). All together, these results demonstrate that conjugation of a CpG oligonucleotide to α-tocopherol altered its biodistribution. We observed an accumulation of Toco-PO-CpG oligonucleotide in secondary lymphoid tissues and, importantly, the route of administration plays a pivotal role in defining preferential localization organs. When Toco-PO-CpG oligonucleotides were administered SC, the compounds mostly accumulated in draining LNs, while IV administration resulted in localization of these oligonucleotides in spleens. Flow cytometry analysis revealed that, in lymphoid organs, labeled Toco-PO-CpG oligonucleotides were associated with TLR9-expressing cells, such as $CD11c^+$ DCs, $F4/80^+$ macrophages, and B cells (Figures 4E and 4F). Because liver is a major organ for oligo accumulation, we also examined the accumulation of AF647-labeled Toco-PO-CpG and PO-CpG in other major organs of oligonucleotides distribution, such as liver and kidney (Figure S6). We found greater signal for Toco-PO-CpG compound in these organs compared with its unconjugated counterpart, likely due to the low-density lipoprotein (LDL) particles binding and receptor-mediated endocytoses.[16] This observation is in good general agreement with previously reported finding for other antisense lipids, such as cholesterol- and tocopherol-conjugated oligonucleotide constructs.[21]

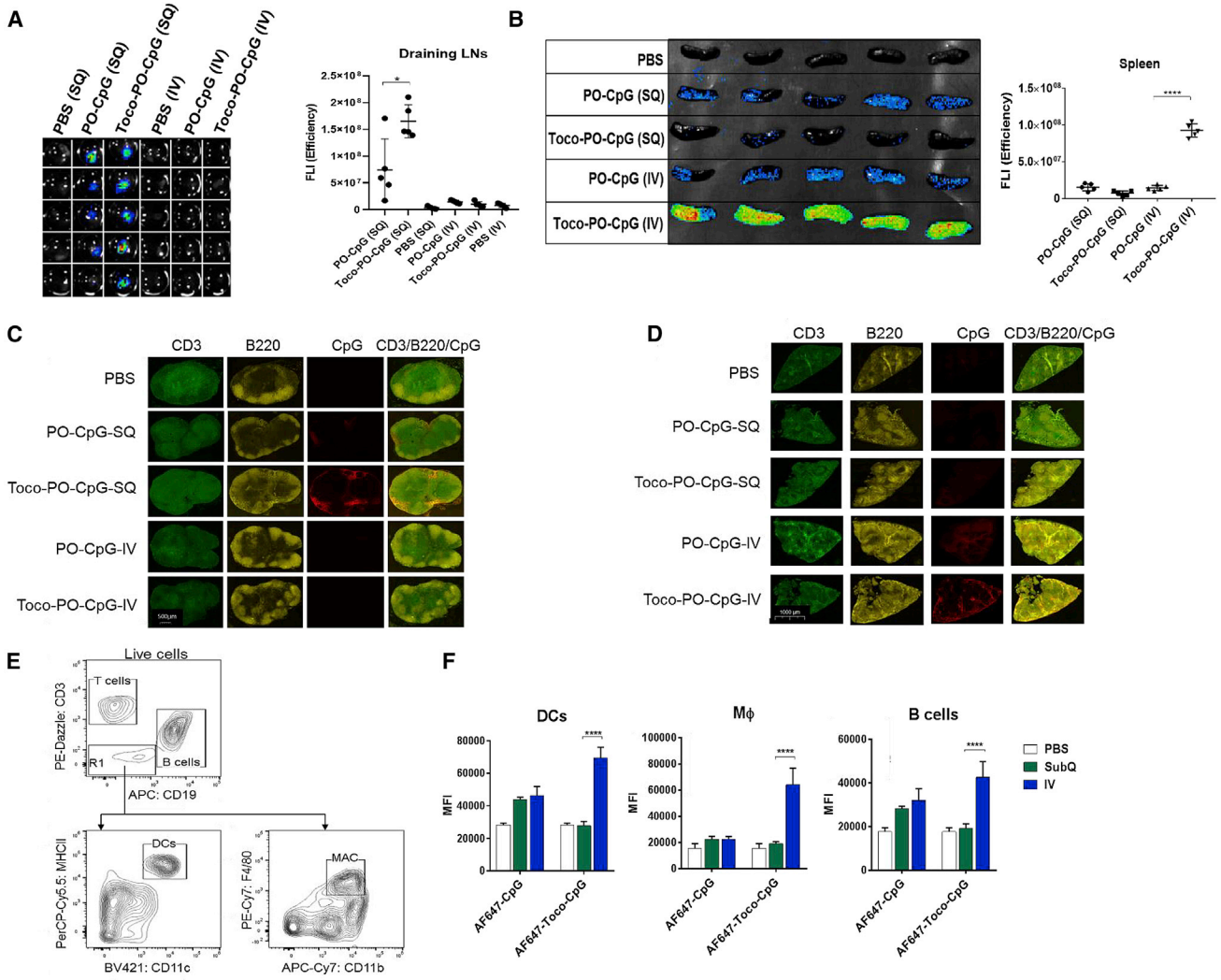

Figure 4. Trafficking of α-tocopherol-conjugated CpG oligonucleotides to secondary lymphoid organs

(A) IVIS fluorescence imaging and quantification of excised draining LNs from C57BL/6 mice (n = 5) 24 h post injection with fluorescein-labeled CpG oligonucleotides. (B) IVIS fluorescence imaging and quantification of excised spleens from C57BL/6 mice (n = 5) 24 h post injection with AF647-labeled CpG oligonucleotides. (C and D) Immunohistochemistry of draining LNs (C) and spleens (D) 24 h post injection with AF647-labeled CpG oligonucleotides. (E and F) The uptake of fluorescently labeled CpG oligonucleotides by splenic APCs was determined by flow cytometry at 24 h post injection. ****p < 0.0001, ***p < 0.001, **p < 0.01, *p < 0.05.

α-Tocopherol conjugation of CpG oligonucleotides increases humoral response in mice immunized with HBsAg

To assess whether the preferential delivery of Toco-PO-CpG oligonucleotides to lymphoid organs alters the adaptive immune response to an antigen, we immunized mice via either SC or IV routes with recombinant hepatitis B surface antigen (HBsAg), either alone or in combination with the CpG oligonucleotides. Two weeks later, the immune response was boosted by re-immunizing mice with the same set of compounds as the ones used during the priming phase. Production of antibodies specific for HBsAg were determined by enzyme-linked immunosorbent assay (ELISA) 2 weeks after the boost immunization. When recombinant HBsAg was immunized with Toco-PO-CpG oligonucleotide, we observed significantly higher humoral immune responses in comparison with its unconjugated counterpart (PO-CpG) (Figure 5A), indicating that the α-tocopherol moiety enhanced antigen-specific IgG response due to preferential TLR9 activation in secondary lymphoid organs. Unexpectedly, the antibody titer was up to 3-fold higher in sera of mice that received HBsAg combined with Toco-PO-CpG administered IV compared with SC administration ($p < 0.01$) (Figure 5A). No statistically significant differences between the two different administration routes were observed in mice receiving PS-CpG or PO-CpG as adjuvants, although the trend was higher in IV groups (Figure 5A). These results suggest that the magnitude of the humoral immune response strongly correlates with the preferential localization of CpG oligonucleotides to secondary lymphoid organs.

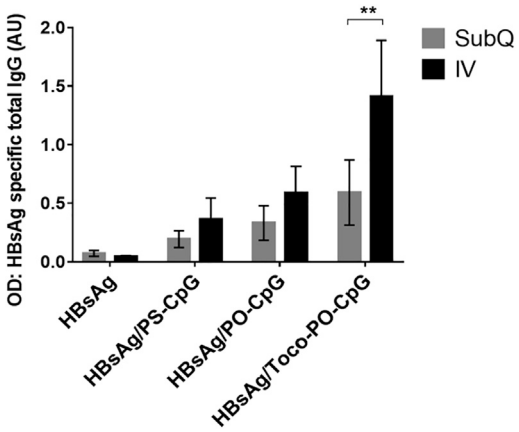

Figure 5. Usage of Toco-PO-CpG oligonucleotides as adjuvant induces more potent humoral immune response

C57/Bl6 mice (n = 5) were immunized either IV or SC with HBsAg alone or in combination with Toco-PO-CpG or unconjugated control CpG oligonucleotides on days 0 and 14. HBsAb titer in serum was determined by ELISA 30 days after initial immunization. **p < 0.01.

In vivo antiviral activity of CpG oligonucleotides in AAV/HBV mouse model

In human clinical trials, the HBV vaccine Engerix-B with CpG oligonucleotide adjuvant demonstrated significant improvement over conventional vaccine containing alum adjuvant.[14,22,23] Previously, Yang et al. demonstrated in mice using the AAV/HBV model that, when combined with a CpG oligonucleotide, Engerix-B could be used as a therapeutic vaccine.[24] There are multiple mouse models to study HBV, each reflecting important aspects of the human CHB disease. In the AAV/HBV model, mice infected with AAV/HBV establish persistent viremia for more than 30 weeks and exhibit immune tolerance when prophylactically immunized with the conventional vaccine containing aluminum adjuvant similar to that observed in CHB-affected patients.[24–26] It was shown that immunization with the Engerix-B/CpG oligonucleotide combination resulted in generation of humoral and cellular immunity directed against HBV and significantly reduced HBV viral load. We reasoned that, because IV administration of Toco-PO-CpG-conjugated oligonucleotide had enhanced activity and favorable biodistribution compared with SC administration, it could be used as an immunomodulator in the AAV/HBV mouse model. Mice were injected IV with 1×10^{11} viral genomes of AAV/HBV and were allowed to establish a stable infection. Forty-five days after infection, mice with stable viral load were grouped and treated with compounds. We dosed mice IV or SC with either Toco-PO-CpG or the parent PO-CpG oligonucleotides. In previous experiments, it was observed that a single dose of CpG oligonucleotides could lower viral load, but the effect was not durable (data not shown). We treated the infected mice with multiple doses of CpG oligonucleotides every other week over 98 days, then monitored viral load for an additional 4 weeks to evaluate the duration of the immune responses while the mice were off treatment (Figure 6A). Mice treated with either PO-CpG or Toco-PO-CpG oligonucleotides experienced a significant decline in serum HBV DNA and HBsAg levels (Figures 6B and 6C); however, hepatitis B e antigen (HBeAg) remained unchanged (Figure S7). Repeated administration of the CpG oligonucleotides caused further significant decrease in circulating HBV DNA and HBsAg, relative to vehicle-treated mice. On day 63, 1 week after receiving five doses of the Toco-PO-CpG oligonucleotides, circulating levels of HBV DNA and HBsAg were near the lower limit of detection (LLOD). Further dosing until day 98 sustained circulating levels of HBV DNA and HBsAg below the LLOD, which represented an over 3-log drop in circulating HBsAg and over 2-log drop in circulating HBV DNA levels. In contrast, although multiple doses of PO-CpG oligonucleotides also resulted in significant decline of circulating HBV DNA and HBsAg, mice receiving the unconjugated PO-CpG oligonucleotides failed to reduce these markers to undetectable levels. On average, HBsAg was reduced over 2-log and HBV DNA was reduced over 2-log (Figures 6B and 6C). HBeAg was significantly reduced after multiple doses; however, it remained detectable in circulation (Figure S7).

To measure the humoral response, mice were monitored weekly for circulating levels of anti-hepatitis B surface antibody (HBsAb). Seroconversion to HBsAb was observed in all mice with Toco-PO-CpG. In contrast, none of the PBS-treated mice developed anti-HBsAb and only five out of 10 PO-CpG-treated mice developed anti-HBsAb above the LLOD (170 IU/mL). Interestingly, the kinetics of the anti-HBsAb response in Toco-PO-CpG-treated mice were faster than in mice treated with the parent PO-CpG. The mean anti-HBsAb response in Toco-PO-CpG-treated mice is detectable above the LLOD by day 63 (Figure 6D). However, in mice treated with PO-CpG, on average, the anti-HBsAb response is significantly above PBS-treated mice by day 63 but does not surpass the LLOD except during the peak of the humoral response at day 105. Moreover, the magnitude of the humoral response was significantly greater in Toco-PO-CpG-treated mice compared with the mice receiving parental compound. As shown in Figure 6D, on day 105, at the peak of the measured response, mice receiving Toco-PO-CpG had over 5-fold concentration of serum anti-HBsAb compared with the mice receiving parental compound (1,189.71 mIU/mL ± 113.94 versus 216.17 ± 28.84 mIU/mL, $p < 0.01$).

To test for induction of HBV-specific splenocytes, approximately 1 month after the last treatment, AAV/HBV-infected mice were sacrificed and splenocytes from individual mice were incubated in the presence or absence of HBV-specific epitopes. When incubated with HBsAg epitopes, Toco-PO-CpG- and PO-CpG-treated mice had significantly more IFN-γ-producing splenocytes than the PBS-treated mice (217.5 ± 57.1 and 49.5 ± 11.5 SFC/10^6 splenocytes respectively) (Figure 6E). This result was reproducible, but the magnitude of the response varied between experiments. Taken together, these results demonstrate that targeting CpG oligonucleotide to lymphoid organs enhances their potency in stimulating humoral and cellular immunity, resulting in improved protection against HBV.

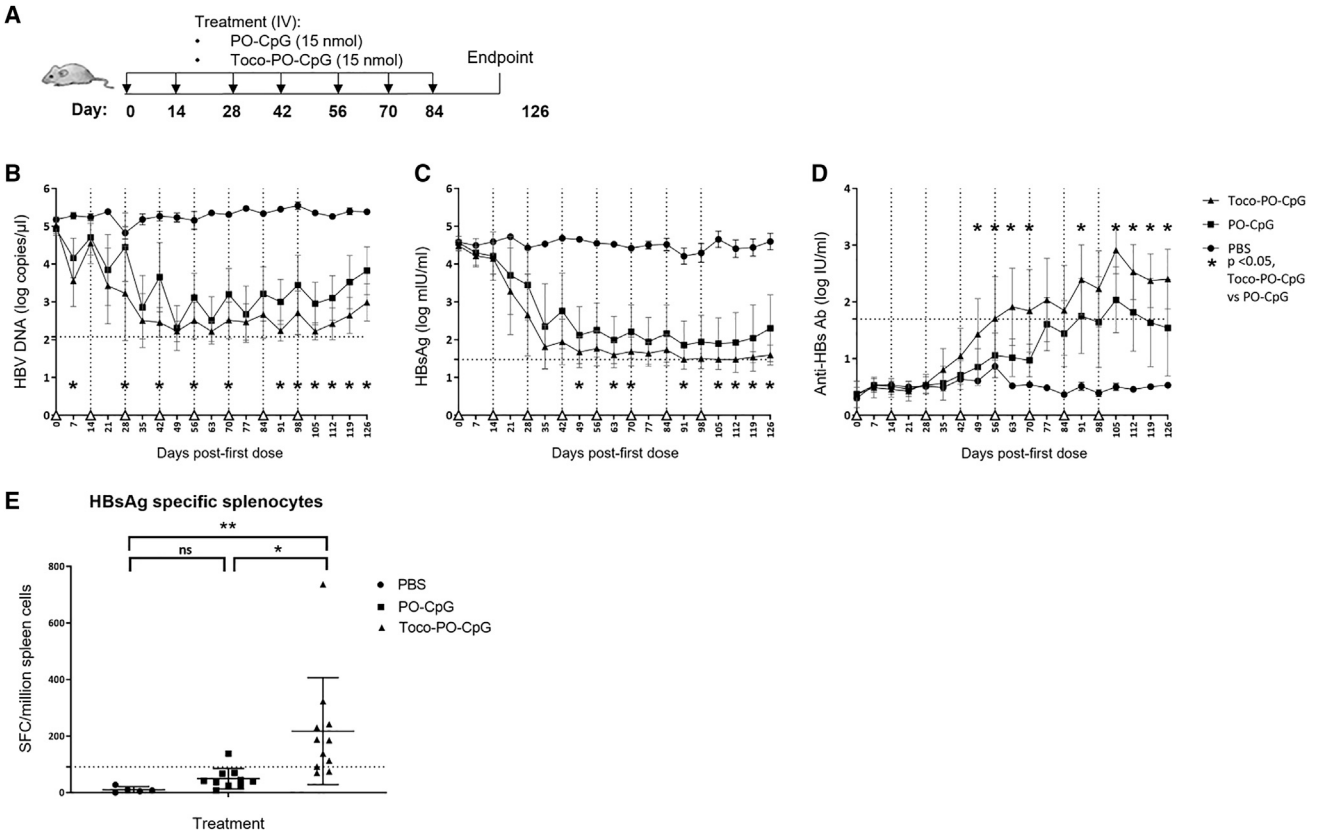

Figure 6. Toco-PO-CpG treatment results in viral clearance in AAV/HBV-infected mice

(A) Schematic presentation of treatment schedule. AAV/HBV-infected C57/Bl6 mice (n = 10) were dosed IV with either PO-CpG or Toco-PO-CpG (15 nmol/animal) every other week until day 84. Afterward, animals were monitored for 4 weeks with the experimental endpoint at day 126.

(B) HBV genomic DNA in the serum was determined by real-time PCR. (C) Serum HBsAg levels in the different groups were monitors by ELISA (n = 5); LLOD 148 IU/mL. (D) HBsAb titers were measured by ELISA; LLOD 170 IU/mL. (E) IFN-γ production by splenocytes at the end of treatment. Splenocytes were freshly isolated, stimulated with a pool of 15-mer overlapping HBsAg epitopes, and the quantity of IFN-γ-producing cells was measured by ELISpot. The error bars represent SD. $^{**}p < 0.01$, $^{*}p < 0.05$.

DISCUSSION

Our goal in this study was to modify the structure of the oligonucleotide to potentiate its activity and to enable preferential tissue targeting. Based on the crystal structure of TLR9 bound to an agonist CpG oligonucleotide, Ohto et al. described that, in addition to the receptor forming important contacts with the bases of the CpG motif, the receptor also interacted with the sulfur atom of the PS backbone. We reasoned that reverting the PS to its native PO at the backbone bridging the CpG motif would have a positive impact on ligand interaction. Interestingly, substituting two of the four CpG motifs in ODN 7909, at cytidines number 5 and 13 (C^5 and C^{13}), had a dramatic effect in potentiating activity of the oligonucleotide, whereas substituting PO at the backbone of either or both other CpG motifs, at C^2 and C^{21}, did not affect the activity significantly. In the course of conducting these experiments, Pohar et al. made a similar observation that reversion of PS to PO at the two CpG motifs in a prototypic CpG oligonucleotide, ODN-H75, increased its efficacy.[27]

Previously, it has been shown that the conjugation of CpG oligonucleotides to tissue targeting moieties leads to enhanced activity. Radovic-Moreno et al. conjugated a prototypic mTLR9 agonist ODN 1826 to tocopherol and showed that this modification enhanced oligonucleotide potency *in vitro*. The authors attributed this enhanced activity to the ability of the conjugated molecule to self-aggregation into a quaternary structure.[12] Using a synthetic lipid conjugated to a CpG oligonucleotide, Liu et al. demonstrated that, in addition to assembling into micellar structures, the conjugated oligo could bind to albumin. This property enhanced distribution of the oligonucleotides to lymphoid organs.[13] In this report, we describe that conjugating a PO-optimized oligonucleotide to α-tocopherol via a cleavable linker can potentiate its activity *in vitro* and *in vivo*. Toco-PO-CpG can assemble into micelle-like structures and bind to albumin, and these two properties enhance its uptake into cells, and distribution to lymphoid tissues. Notably, the nature of the linker bridging α-tocopherol and the oligonucleotide was critical. We found that, for the oligonucleotide to become fully active, the linker needed to be conjugated to the oligonucleotide via a PO linkage. Substitution of this group to PS markedly diminished the activity. We hypothesize that, once internalized, the α-tocopherol and linker are cleaved from the oligonucleotide within the endosome.

The ability of Toco-PO-CpG to self-assemble into micelle-like structures and its ability to bind albumin explain its enhanced activation efficiency. Using a fluorescent-labeled version of Toco-PO-CpG, we observed accelerated kinetics of uptake by cell lines and primary cells. We hypothesize that because the oligonucleotides are assembled in a quaternary structure, this complex is more efficiently endocytosed into cells by lipoprotein receptors. *In vivo*, α-tocopherol conjugation clearly affected biodistribution of the CpG oligonucleotide. We demonstrated preferential delivery of α-tocopherol-conjugated oligonucleotides to secondary lymphoid tissues. We compared two administration routes (IV and SC) and found that IV administration of tocopherol-conjugated oligonucleotide resulted in its accumulation in spleen, whereas SC administration leads to oligonucleotide delivery to draining LNs. Liu et al. demonstrated that a synthetic lipid-conjugated CpG bound to albumin, and albumin was preferentially distributed to the secondary lymphoid organs.[13] It is likely that α-tocopherol binding to albumin results in the same effect.

By increasing the efficiency of oligonucleotide delivery to secondary lymphoid tissues, we observed potent enhancement of its efficacy in multiple immunization models. In an adjuvant model using recombinant antigen, the Toco-PO-CpG oligonucleotide was much more effective at inducing an antigen-specific humoral response than its parent compound, PO-CpG. Because α-tocopherol conjugation enhanced oligonucleotide delivery to secondary lymphoid tissues and increased uptake into APCs, we believe that these factors can account for the enhanced efficacy. IV delivery of HBsAg mixed with Toco-PO-CpG achieved a 3-fold increase in antibody titer over that of the parent compound, highlighting the effect of efficiently delivering the Toco-PO-CpG oligonucleotide to the spleen. Within the spleen, the predominance of TLR9-responsive B cells and innate immune cells was efficiently stimulated by Toco-PO-CpG oligonucleotide and HBsAg to mount a vigorous humoral response.

Based on the compelling *in vitro* and *in vivo* data demonstrating the enhanced functional activity of the Toco-PO-CpG oligonucleotide, we tested it as a single-agent therapy in AAV-HBV-infected mice. TLR9 agonists have been previously shown to be effective in mouse models of HBV.[24,28] AAV-HBV-infected mice resemble chronic HBV infection in that the immune system is tolerized against HBsAg. Yang et al. used the prototypic mTLR9 agonist CpG oligonucleotide (ODN 1826) as an adjuvant when administered with Engerix-B. Interestingly, from a single dose of ODN 1826 and Engerix-B, and then boost with Engerix-B, the mice were able to mount an effective humoral and cytotoxic response.[24] As a single-agent therapy, our Toco-PO-CpG oligonucleotide, but not the parent PO-CpG oligonucleotide, was highly effective at inducing humoral and cellular immunity and ultimately reducing viral load. Therapeutic dosing consisted of biweekly injections of Toco-PO-CpG oligonucleotide. After five to six injections, circulating levels of HBV DNA and HBsAg for most mice were below LLOD. In addition, on average, after the fifth injection, Toco-PO-CpG oligonucleotide-treated mice had detectable levels of α-HBsAg antibody and levels increased following subsequent doses. Eventually, by the end of the study, all mice treated with Toco-PO-CpG oligonucleotide had detectable levels of α-HBsAg antibody. The induction of a humoral response against HBsAg correlated with diminished levels of circulating HBsAg, and, after the seventh dose, all mice treated with Toco-PO-CpG oligonucleotide had undetectable circulating levels of HBsAg. After the last treatment, we monitored the mice for 1 month and we observed that all mice were able to maintain near-undetectable levels of HBsAg. Furthermore, at the end of the study, we detected HBsAg-specific splenocytes in nearly all mice on the study.

It is widely believed that high levels of circulating HBsAg are immunosuppressive.[29,30] The AAV-HBV model appears to resemble this aspect of CHB infection because untreated, infected mice do not develop either a humoral or cellular response against HBV antigens. Yang et al. were able to overcome tolerance to HBsAg by using CpG in conjunction with a HBsAg vaccine, Engerix-B. In this report, we demonstrate that, through repeat injections of Toco-PO-CpG oligonucleotide, we were able to overcome tolerance to HBsAg and induce both humoral and cellular immunity to HBV that were able to reduce viral load. In contrast, the parent PO-CpG oligonucleotide was partially effective in activating the immune response and, as a result, was ineffective at reducing viral load. The ability to preferentially deliver the CpG oligonucleotide to secondary lymphoid tissues clearly had a positive effect on controlling HBV in this disease model.

We demonstrated that structural modifications to the prototypic TLR9 agonist oligonucleotide ODN 7909 were able to potentiate its immunostimulatory functions. By reverting the bridging PS groups to PO in the CpG motifs and by conjugating α-tocopherol via a cleavable linker, the resulting construct had superior potency, enhanced cellular uptake, and efficient biodistribution to secondary lymphoid organs. These enhanced capabilities improved its immunomodulatory function and were effective in therapeutic treatment as a single agent in the AAV/HBV model of chronic HBV infection. We present a promising strategy for designing a novel class of TLR9 agonists that can be used as potent immunomodulatory therapeutics in treating chronic diseases in which the immune response directed against diseased cells is profoundly suppressed.

MATERIALS AND METHODS

Oligonucleotide synthesis

All oligonucleotides were synthesized on ABI 394, or Expedite 8909, or GE Healthcare ÄKTA Oligopilot Plus 100 Synthesizers. The synthesis was carried out on 1–150 μmol scale in a 3′ to 5′ or 5′ to 3′ direction with the corresponding phosphoramidite monomers. Tocopherol phosphoramidite was purchased from ChemGenes corporation (CLP-2706). Cleavage from the support and removal of base- and phosphorus-protecting groups was achieved by treatment with concentrated aqueous ammonium hydroxide solution for 8 h at 55°C or 1:1 ammonium hydroxide:methyl amine (AMA) solution at room temperature (RT) for 3 h or at 65°C for 15 min.

The unconjugated oligonucleotides were purified by high-performance liquid chromatography (HPLC) using DNAPac PA-100

column with 20 mM sodium phosphate in 10% acetonitrile, pH 8 as mobile phase A (MPA), and 20 mM sodium phosphate in 10% acetonitrile, 1.8 M sodium bromide, pH 8 as mobile phase B (MPB). Tocopherol-conjugated oligonucleotides were purified by a reverse phase HPLC column (Sepax GP-C8 column) using 50 mM sodium acetate in 10% acetonitrile (MPA) and 100% acetonitrile (MPB). Fractions containing full-length oligonucleotide product were pooled, desalted, and lyophilized.

Final oligonucleotide purity and identity was confirmed by liquid chromatography-mass spectrometry (LC-MS; Ultimate 3000 HPLC coupled to LTQ-XL ion trap). A C_{18} column (Acquity BEH 2.1 × 50 mm, 1.7 μm from Waters, Milford, MA) with MPA: 100 mM hexafluoroisopropanol (HFIP), 7 mM TEA, and MPB: 70% methanol, 30% acetonitrile. A gradient of 2%–25% MPB in 7 min was used for the unconjugated oligonucleotide. The conjugated oligonucleotides were analyzed by a C_8 column (Acquity BEH 2.1 × 50 mm, 1.7 μm from Waters, Milford, MA) with MPA, 100 mM HFIP, 7mM TEA; MPB, acetonitrile; and a 15%–55% gradient of MPB in 7 min. Flow rate and column temperature were 0.3 mL/min and 60°C, respectively. Full-scan mass spectra were acquired in negative ion mode using Xcalibur software. Final-sample endotoxin level was analyzed using Endosafe-nexgen-PTS (Charles River).

Cell lines

HEK-Blue mTLR9, hTLR9, hTLR2, hTLR3, hTLR4, hTLR5, hTLR7, and hTLR8 (InvivoGen), which stably express a secreted alkaline phosphatase (SEAP) inducible by NF-κB, were cultured as recommended by the supplier. Human PBMCs (ATCC) were isolated from fresh peripheral blood collected from healthy donors.

HEK-Blue TLR reporter cell lines

To screen and characterized TLR agonists, we utilized HEK293-derived HEK-Blue TLR reporter cell lines obtained from InvivoGen. Cells were cultured in accordance with manufacturer's instructions, and assays were optimized to ensure appropriate positive control performance. Briefly, cells were maintained in DMEM, 4.5 g/L glucose media supplemented with 2 mM glutagro, 100 U/mL penicillin, 100 μg/mL streptomycin (all from Corning, NY), 10% heat-inactivated (HI) fetal bovine serum (FBS) (Sigma), 100 μg/mL Normocin (InvivoGen), and appropriate selective antibiotics. Compound dilutions were prepared in culture media and added to the culture plates prior to cell seeding. Cells were cultured with compounds for 16–24 h at 37°C in 5% CO_2. To measure production of SEAP, 20 μL of culture supernatant were transferred into 180 μL of Quanti-Blue detection medium (InvivoGen), incubated for 2–6 h at 37°C, and measured at optical density (OD) 630 nm using Victor X3 plate reader (PerkinElmer). Post-assay viability of HEK-Blue cells was determined following 4–6-h incubation with alamarBlue (Bio-Rad) by measuring fluorescence (560 nm excitation, 590 nm emission) on Victor X3 plate reader (PerkinElmer). EC50s of SEAP expression were calculated in Prism 8 (GraphPad) based on triplicates expressed as percentage of maximum activation by the positive control, typically 2 μM ODN 2006 (InvivoGen).

SEC

SEC was performed on an Ultimate 3000 HPLC (Thermo Scientific) equipped with a Superdex 75 Increase (GE Healthcare). Samples of oligonucleotides at 1–5 μM concentration in the presence or absence of urea (for the micelle formation study) or BSA (in protein binding study) were injected on the column. A solution of 1× PBS, 20 mM KCl, at a flow rate of 0.075 mL/min at RT was used to elute the samples from the column, the chromatogram was recorded at 260 or 500 nm, and emission was recorded at 525 nm (500 nm was used for excitation).

HBsAg immunizations

C57BL/6 male mice, 6–8 weeks old (Envigo) were vaccinated by a homologous prime-boost regimen; animals were primed on day 0 and boosted on day14 with HBsAg (5 μg) (Janssen Vaccines, Korea) alone or in combination with CpG oligonucleotides (30 nmol) in a total volume of 100 μL. Vaccine mixing was performed in PBS buffer. Injections of CpGs were performed either SC between the shoulder blades or IV into the tail vein.

ELISA for HBsAg

Nunc clear flat-bottom immune plates (Thermo Fisher) were coated with 5 μg/mL HBsAg recombinant protein in PBS buffer and incubated overnight at 4°C. The plates were blocked with 2% BSA in PBS once and washed four times with ELISA wash buffer (PBS with 0.05% Tween 20). Mouse serum was diluted in blocking buffer and incubated on the plate for 2 h at RT, followed by four washes. Secondary HRP-conjugated antibody was diluted 1:1,000 in blocking buffer and incubated on plate for 2 h, followed by four washes. TMB substrate (KPL) was applied to the plate and the reaction was stopped with 2 N sulfuric acid. The absorbance was measured at 450 nm.

In vitro CpG oligonucleotide cellular uptake

AF647 conjugated CpG oligonucleotides (1 μM) were incubated with the InvivoGen HEK-Blue human cell line for 15 min, 30 min, 1 h, 2 h, 4 h, 6 h, and 24 h. Cells were then stained with LIVE/DEAD fixable aqua dead cell dye (Thermo Fisher) and uptake was quantified using the MFI of viable cells by FACS.

Flow cytometry

All antibodies were purchased from BioLegend. The following primary antibodies were used: anti-CD16/CD32 (clone: 93), anti-CD3-PE/Dazzle 594 (clone: 17A2), anti-CD19-APC (clone: 6D5), anti-MHCII-PerCP/Cy5.5 (clone: M5/114.15.2), anti-CD11c-BV421 (clone: N418), anti-F4/80-PE/Cy7(clone: BM8), anti-CD11b-APC/Cy7 (clone: M1/70), anti-CD86-BV605 (clone: GL-1), and anti-CD40-FITC (clone: 3/23).

IVIS

For *in vivo* imaging, C57Bl/6 male mice between 7 and 8 weeks old were used. All animal experiments were performed in compliance with the Institutional Animal Care and Use Committee (IACUC) protocols. Twenty-four hours after the injection of AF647-labeled CpG oligonucleotides (15 nmol per animal), animals were sacrificed

and spleens and draining LNs were excised and imaged using the IVIS Spectrum Imaging System (Ami HTX). An image set (Ex, 605 nm; Em, 670 nm; f 5; 10 s) was collected. Spectral Instruments Imaging Software Aura was used to acquire and quantitate the fluorescence imaging datasets. A region of interest tool was used to measure the radiant efficiency from each organ.

IF

Twenty-four hours after injection of AF647-labeled CpG oligonucleotides (15 nmol per animal), animals were sacrificed and spleens and draining LNs were excised. IF was performed using Leica Bond automated immunostainer on formalin-fixed paraffin-embedded (FFPE) mouse lymph node and spleen. Heat-induced antigen retrieval was performed using Leica Bon Epitope Retrieval Buffer 2 (EDTA solution, pH 9.0) for 20 min. Staining was performed with an overnight incubation for primary antibodies, a rat anti-CD45R (B220) (RA3-6B2), eFluor 570 antibody (Thermo Fisher), and rabbit anti-CD3 antibody (Abcam). A secondary antibody, goat anti-rabbit IgG Alexa Fluor Plus 488 (Thermo Fisher) was applied and slides were mounted with DAPI in Fluorogel II for nuclear visualization.

Animals for AAV/HBV studies

Male C57BL/6 mice, 5 weeks old, specific pathogen free, were obtained from Shanghai Laboratory Animal Center (SLAC) (Shanghai, China). The mice were housed in the animal care facility in individually ventilated cages after the animals arrived at the WuXi AppTec animal facility. The study was approved by the WuXi Institutional Animal Care and Use Committee (IACUC; protocol N20160810-Mouse). The mice acclimated to the new environment for 4 days before the start of the study.

Efficacy study in rAAV/HBV transduced mice

Mice were injected via the tail vein with 200 μL of PBS solution containing 1×10^{11} v.g./mice of rAAV8-1.3HBV, genotype D virus (FivePlus). After 8 weeks of infection, mice with qualified viral load (HBV DNA >5 Log copy/mL, HBsAg >4 Log IU/mL, HBeAg >3 Log PE IU/mL) were selected and randomly grouped with five mice per group (no significant difference in viral markers among groups). Toco-PO-CpG or PO-CpG oligonucleotides (30 nmol/animal) were administered either IV or SC every other week for 14 weeks (day 0 is defined as the day of dosing). They were followed up for 4 weeks after the end of treatment. At the end of treatment and follow-up, mice were euthanized and bled via cardiac puncture for preparation of plasma and blood cells.

HBV viremia level in mouse plasma

HBV DNA in the mouse plasma was isolated with the QIAamp 96 DNA Blood Kit (Qiagen) following the manufacturer's manual, and then quantified by qPCR with FasStart Universal Probe Mast(ROX) (Roche) on ABI Prism 7900HT (Applied Biosystems). The DNA samples were analyzed by real-time qPCR using HBV-specific primers (HBV forward primer, 5′-GTGTCTGCGGCGTTTTATCA-3′; HBV reverse primer, 5′-GACAAACGGGCAACATACCTT-3′) and HBV probe (FAM-CCTCTKCATCCTGCTGCTATGCCTCATC-TAMRA). The primers and probe were synthesized by Genwiz (Suzhou) and Sangon (Shanghai). HBsAg, HBeAg, and anti-HBsAb levels in plasma were detected using the HBsAg ELISA kit (Autobio), HBeAg ELISA kit (Autobio), and anti-HBs detection kit (Autobio), respectively, following the manufacturer's manuals.

Cytokine measurement

Cytokine and chemokine concentrations were measured using MILLIPLEX Mouse Premixed 32-plex (Millipore) according to the manufacturer's instructions. The cytokines chosen for analysis were IFN-γ, IL-12p40, TNF-α, IL-6, IL-1β, MCP-1, IL-10, and IP-10. In addition, IFN-α was measured by Procartaplex Mouse IFN-α Simplex (Invitrogen) according to the manufacturer's instructions.

IFN-γ ELISpot assay

Spleens were weighed and collected in RPMI 1640 medium supplemented with 1% penicillin-streptomycin and 5% FBS (Hyclone) for isolation of mononuclear cells. Single-cell suspensions were prepared from spleens through cell strainer followed with red blood cell lysis by 1xRBC Lysis buffer solution (eBioscience). IFN-γ ELISpot assay were performed following the manufacturer's instructions of Mouse IFN-gamma ELISpot BASIC (ALP) kit (Mabtech). Briefly, Millipore 96-well nitrocellulose plates were precoated with 100 μL/well (15 μg/mL) anti-IFN-γ monoclonal antibody (mAb) at 4°C overnight. The plates were washed five times with PBS and blocked in complete RPMI 1640 medium with 10% FBS for 30 min at 37°C. Excess coating antigen was removed and 2×10^5 cells/well splenocytes in single-cell suspension (in 50 μL volume) were seeded with or without 50 μL(2 μg/mL) of overlapping peptides of HBV consensus B, C, and D, 15-mer overlapped by 11 amino acid, or individual known HBV epitopes of core and surface. The plates were incubated for 20 h at 37°C. To detect spots, cells were removed, and plates were washed five times with PBS, and 100 μL/well of R4-6A2-biotin (μg/mL) in PBS with 0.5% FBS was added to the wells and the plates were incubated for 2 h at RT. The plates were then washed five times with PBS and 100 μL of streptavidin-ALP diluted 1:1,000 in PBS with 0.5% FBS was added to the wells and incubated at RT for 1 h. To develop the spots, plates were washed five times in PBS and 100 μL of BCIP/NBT plus substrate was added to wells and incubated for 10 min at RT. The reaction was stopped by emptying the plates and washing extensively in water. The plates were air dried overnight and colored spots were enumerated in a CTL-FluoroSpot Analyzer.

Statistical analysis

Statistical analyses were performed using a two-tailed unpaired t test and Prism software (GraphPad Software, San Diego, CA), and $p < 0.05$ was considered statistically significant.

SUPPLEMENTAL INFORMATION

Supplemental information can be found online at https://doi.org/10.1016/j.omtn.2022.01.020.

ACKNOWLEDGMENTS

The authors thank Janssen Biopharma Research for supporting this work, Navdeep Bilon for oligonucleotide synthesis support, and Yi

Jin for meaningful discussion and program support. We also thank Puja Ravikumar and Jan Rydzewski at Molecular Medicine Research Institute for their *in vivo* study support and expertise.

AUTHOR CONTRIBUTIONS

I.U., S.M.G., and T.Y. conceived the main conceptual idea, and designed and directed the project. I.U. wrote the manuscript with support from T.Y. and S.M.G. All authors discussed the results and contributed to the final manuscript. I.U. designed, performed, and interpreted HBsAg immunization and *in vivo* imaging studies. E.R. performed *in vitro* assays with HEK-Blue TLR reporter cell lines. She also measured cytokine release in PBMCs post treatment with TLR9 agonists. R.Z., Q.H., and C.L. carried out AAV/HBV *in vivo* studies. R.Z. performed IFN-γ ELISpot assay. Q.H. determined HBV viremia level in mouse plasma. N.T.S.D.C. and R.K.P. carried out oligonucleotide synthesis as well as conjugation of oligonucleotides to fluorophores and/or lipid moieties. S.P. designed, performed, and analyzed SEC studies. L.B., S.M.G., and T.Y. developed the theoretical framework, provided critical feedback, and helped shape the research.

DECLARATION OF INTERESTS

The authors declare no competing interests.

REFERENCES

1. Lee, W.M. (1997). Hepatitis B virus infection. N. Engl. J. Med. *337*, 1733–1745.
2. Lai, C.L., Chien, R.N., Leung, N.W., Chang, T.T., Guan, R., Tai, D.I., Ng, K.Y., Wu, P.C., Dent, J.C., Barber, J., et al. (1998). A one-year trial of lamivudine for chronic hepatitis B. Asia Hepatitis Lamivudine Study Group. N. Engl. J. Med. *339*, 61–68.
3. Hoofnagle, J.H., and Lau, D. (1997). New therapies for chronic hepatitis B. J. Viral Hepat. *4*, 41–50.
4. Rehermann, B., and Nascimbeni, M. (2005). Immunology of hepatitis B virus and hepatitis C virus infection. Nat. Rev. Immunol. *5*, 215–229.
5. Wherry, E.J., Barber, D.L., Kaech, S.M., Blattman, J.N., and Ahmed, R. (2004). Antigen-independent memory CD8 T cells do not develop during chronic viral infection. Proc. Natl. Acad. Sci. U S A *101*, 16004–16009.
6. Raziorrouh, B., Schraut, W., Gerlach, T., Nowack, D., Grüner, N.H., Ulsenheimer, A., Zachoval, R., Wächtler, M., Spannagl, M., Haas, J., et al. (2010). The immunoregulatory role of CD244 in chronic hepatitis B infection and its inhibitory potential on virus-specific CD8+ T-cell function. Hepatology *52*, 1934–1947.
7. Schurich, A., Khanna, P., Lopes, A.R., Han, K.J., Peppa, D., Micco, L., Nebbia, G., Kennedy, P.T.F., Geretti, A.-M., Dusheiko, G., et al. (2011). Role of the coinhibitory receptor cytotoxic T lymphocyte antigen-4 on apoptosis-Prone CD8 T cells in persistent hepatitis B virus infection. Hepatology *53*, 1494–1503.
8. Pham, E.A., Perumpail, R.B., Fram, B.J., Glenn, J.S., Ahmed, A., and Gish, R.G. (2016). Future therapy for hepatitis B virus: role of immunomodulators. Curr. Hepatol. Rep. *15*, 237–244.
9. Iwasaki, A., and Medzhitov, R. (2004). Toll-like receptor control of the adaptive immune responses. Nat. Immunol. *5*, 987–995.
10. Bode, C., Zhao, G., Steinhagen, F., Kinjo, T., and Klinman, D.M. (2011). CpG DNA as a vaccine adjuvant. Expert Rev. Vaccin. *10*, 499–511.
11. Krieg, A.M. (2008). Toll-like receptor 9 (TLR9) agonists in the treatment of cancer. Oncogene *27*, 161–167.
12. Radovic-Moreno, A.F., Chernyak, N., Mader, C.C., Nallagatla, S., Kang, R.S., Hao, L., Walker, D.A., Halo, T.L., Merkel, T.J., Rische, C.H., et al. (2015). Immunomodulatory spherical nucleic acids. Proc. Natl. Acad. Sci. U S A *112*, 3892–3897.
13. Liu, H., Moynihan, K.D., Zheng, Y., Szeto, G.L., Li, A.V., Huang, B., Van Egeren, D.S., Park, C., and Irvine, D.J. (2014). Structure-based programming of lymph-node targeting in molecular vaccines. Nature *507*, 519–522.
14. Vollmer, J., and Krieg, A.M. (2009). Immunotherapeutic applications of CpG oligodeoxynucleotide TLR9 agonists. Adv. Drug Deliv. Rev. *61*, 195–204.
15. Splawn, L.M., Bailey, C.A., Medina, J.P., and Cho, J.C. (2018). Heplisav-B vaccination for the prevention of hepatitis B virus infection in adults in the United States. Drugs Today *54*, 399–405.
16. Ohto, U., Shibata, T., Tanji, H., Ishida, H., Krayukhina, E., Uchiyama, S., Miyake, K., and Shimizu, T. (2015). Structural basis of CpG and inhibitory DNA recognition by Toll-like receptor 9. Nature *520*, 702–705.
17. Zhang, X.-Y., and Lu, W.-Y. (2014). Recent advances in lymphatic targeted drug delivery system for tumor metastasis. Cancer Biol. Med. *11*, 247–254.
18. Kappus, H., and Diplock, A.T. (1992). Tolerance and safety of vitamin E: a toxicological position report. Free Radic. Biol. Med. *13*, 55–74.
19. Chen, H., Kim, S., Li, L., Wang, S., Park, K., and Cheng, J.-X. (2008). Release of hydrophobic molecules from polymer micelles into cell membranes revealed by Forster resonance energy transfer imaging. Proc. Natl. Acad. Sci. U S A *105*, 6596–6601.
20. Pillai, S.A., Lee, C.-F., Ray, D., Aswal, V.K., Wang, M.-R., Chen, L.-J., and Bahadur, P. (2018). Influence of urea on single and mixed micellar systems of Tetronics®. J. Mol. Liquids *252*, 9–17.
21. Watanabe, A., Nakajima, M., Kasuya, T., Onishi, R., Kitade, N., Mayumi, K., Ikehara, T., and Kugimiya, A. (2016). Comparative characterization of hepatic distribution and mRNA reduction of antisense oligonucleotides conjugated with triantennary N-acetyl galactosamine and lipophilic ligands targeting apolipoprotein B. J. Pharmacol. Exp. Ther. *357*, 320–330.
22. Cooper, C.L., Davis, H.L., Morris, M.L., Efler, S.M., Adhami, M.A., Krieg, A.M., Cameron, D.W., and Heathcote, J. (2004). CPG 7909, an immunostimulatory TLR9 agonist oligodeoxynucleotide, as adjuvant to Engerix-B HBV vaccine in healthy adults: a double-blind phase I/II study. J. Clin. Immunol. *24*, 693–701.
23. Krieg, A.M. (2006). Therapeutic potential of Toll-like receptor 9 activation. Nat. Rev. Drug Discov. *5*, 471–484.
24. Yang, D., Liu, L., Zhu, D., Peng, H., Su, L., Fu, Y.-X., and Zhang, L. (2014). A mouse model for HBV immunotolerance and immunotherapy. Cell Mol. Immunol. *11*, 71–78.
25. Wang, G., Dong, X.-Y., Tian, W.-H., Yu, C.-J., Zheng, G., Gao, J., Wang, G.-J., Wei, G.-C., Zhou, Y.-S., and Wu, X.-B. (2012). [Study on the differences of two mouse models of hepatitis B virus infection by transduction with rAAV8-1. 3HBV]. Bing Du Xue Bao *28*, 541–547.
26. Dong, X.-Y., Yu, C.-J., Wang, G., Tian, W.-H., Lu, Y., Zhang, F.-W., Wang, W., Wang, Y., Tan, W.-J., and Wu, X.-B. (2010). [Establishment of hepatitis B virus (HBV) chronic infection mouse model by in vivo transduction with a recombinant adeno-associated virus 8 carrying 1. 3 copies of HBV genome (rAAN8-1. 3HBV)]. Bing Du Xue Bao *26*, 425–431.
27. Pohar, J., Lainšček, D., Kunšek, A., Cajnko, M.-M., Jerala, R., and Benčina, M. (2017). Phosphodiester backbone of the CpG motif within immunostimulatory oligodeoxynucleotides augments activation of Toll-like receptor 9. Sci. Rep. *7*, 14598.
28. Huang, L.-R., Wohlleber, D., Reisinger, F., Jenne, C.N., Cheng, R.-L., Abdullah, Z., Schildberg, F.A., Odenthal, M., Dienes, H.-P., van Rooijen, N., et al. (2013). Intrahepatic myeloid-cell aggregates enable local proliferation of CD8(+) T cells and successful immunotherapy against chronic viral liver infection. Nat. Immunol. *14*, 574–583.
29. Op den Brouw, M.L., Binda, R.S., van Roosmalen, M.H., Protzer, U., Janssen, H.L.A., van der Molen, R.G., and Woltman, A.M. (2009). Hepatitis B virus surface antigen impairs myeloid dendritic cell function: a possible immune escape mechanism of hepatitis B virus. Immunology *126*, 280–289.
30. Kondo, Y., Ninomiya, M., Kakazu, E., Kimura, O., and Shimosegawa, T. (2013). Hepatitis B surface antigen could contribute to the immunopathogenesis of hepatitis B virus infection. ISRN Gastroenterol. *2013*, 935295.